TECHNISCHE UNIVERSITÄT DRESDEN

Fakultät Elektrotechnik und Informationstechnik

Institut für Akustik und Sprachkommunikation, Lehrstuhl für Akustik und Haptik

Guitar analysis using measurements – X-braced/ E, ρ and G varying

Project partner	Pacific Rim Tonewoods (PRT) 38511 WA-20, Concrete, WA 98237, USA
Contact person	David Olson

Project duration	01.06.2019 – 30.10.2020
Date of report	30.10.2020

Pages of report	30 pages

Contractor	Technische Universität Dresden Fakultät Elektrotechnik und Informationstechnik Lehrstuhl Akustik und Haptik Helmholtzstraße 18 01069 Dresden
Contact person	Sebastian Merchel

1 Introduction

In this report, guitars will be compared regarding their acoustical properties using different measurement approaches. The goal of this comparison is to better understand the physical differences that led to significant preference variation in a previous listening test. Two groups of five guitars each were built. In group one, the density and stiffness of the soundboard and bracewood of the guitar top was varied. In the second group, the soundboard parameters varied but the bracewood was held constant at median values. The guitar labels of the second group are annotated with an apostrophe, e.g., Aa'.

Figure 1 shows some of the varying wood parameters used to build the guitars. Instruments with highest preference in the listening test (marked green) had tops with low density and stiffness. Least preferred were the guitars with high density and stiffness (purple). The coloring scheme introduced in Figure 1 will be used for all measurement plots in this report. The labeling convention with a capital letter for low (A), median (B) or high (C) longitudinal Young's modulus and a small letter for low (a), median (b) or high (c) density will be used.

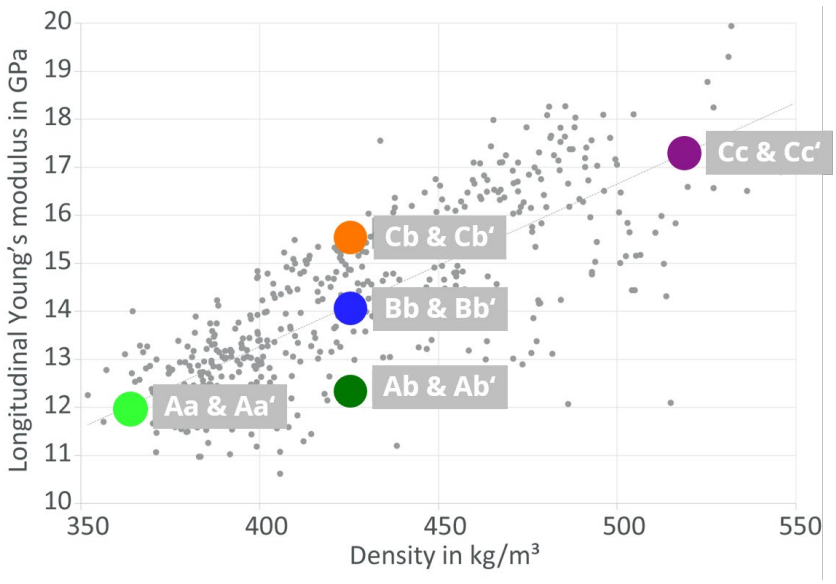

Figure 1 – Schematic representation of soundboard material properties.

Table 1 summarizes the measured material parameters for the soundboard wood used to build the guitars. Additional details can be found in the project report of the first study.

Table 1 – Measured soundboard wood parameters.

Guitar label	Density ρ in kg/m³	Longitudinal Young's modulus E_{LONG} in MPa	Radial Young's modulus E_{RAD} in MPa	Shear G in MPa	Ratio of longitudinal Young's modulus and density
Aa, Aa'	363	12077	1423	506	33.3
Ab, Ab'	415	11436	1692	680	27,6
Bb, Bb'	428	13976	1749	720	32.6
Cb, Cb'	422	15181	1672	727	36,0
Cc, Cc'	518	17380	1959	1269	33.6

For comparison, the results from the listening tests are summarized in Figure 2. It can be seen that the preference ratings in the first group (left) are distributed slightly more homogeneously from worst to best guitar. Specifically, the preference scores for guitars Ab', Bb' and Cb' in the second group (right) appear closer to each other than guitars Ab, Bb and Cb. However, none of the differences between the three guitars in the middle of each group was statistically significant. Nevertheless, the same ranking or tendency is observed in both groups.

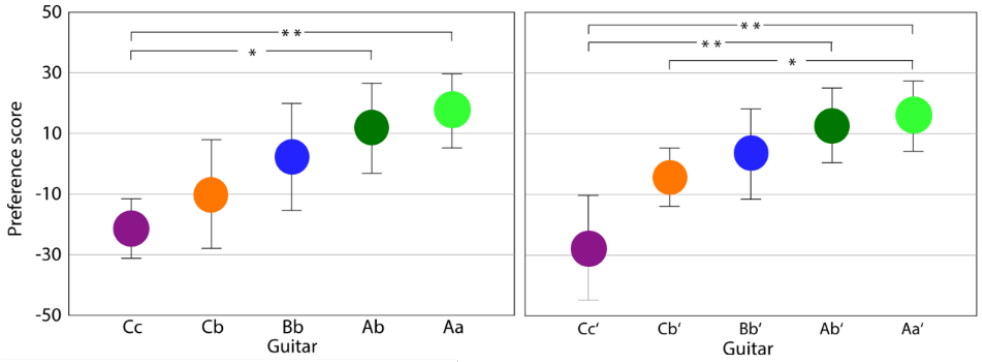

Figure 2 – Summary of the results from previous listening tests.

The reason for the preference of one guitar over another can be multifaceted. Gore and Gilet [1] define a comprehensive list of performance factors including volume, projection, attack, sustain, evenness of loudness between notes, tonal balance, responsiveness in terms of efficiency, dynamic range, timbre as the sound color produced by partials, tonal contrast as the range of producible timbres, separation between individual notes and pitch accuracy. Within the current project, some performance aspects needed to be selected for investigation. Unfortunately, the relative perceptual importance of the factors among themselves in relation to the overall preference for a specific type of instrument is ambiguous. Additionally, the correlation between measurable physical characteristics of an instrument or its radiated sound and the listed performance criteria is not clearly defined.

However, a perceptual test with prerecorded sequences using a homogeneous playing style, as conducted in the previous study, reduces the evaluable performance factors from the perspective of a listener. Most comments during discussions with the guitarists after the listening test referred to differences in the overall tonal balance of the treble middle and bass of the instruments. Therefore, spectral analysis of the recorded sequences and measured transfer functions will be used to attempt to identify some systematic differences between the guitars. Additionally, a modal analysis will help to better understand the vibration behavior of the instruments and temporal aspects will be analyzed using plugged single notes.

2 Sequence analysis

The first approach was to directly search for systematic differences in the recorded music sequences that were used in the listening test. It was expected that guitars with low-density soundboards would be louder than those with heavier tops. However, no systematic difference in overall loudness could be found in the recordings. If mean levels are compared between all recordings, there is a standard deviation of approximately 1 dB. A similar variation was found for repeated recordings of the same instrument, which suggests that the variation in the strength of individual picks and strokes of the guitar player dominate the loudness differences. Figure 3 shows the A-weighted averaged spectra of three strumming sequences used in the listening test for guitars along the diagonal line of Figure 1. A 1/3rd octave smoothing was applied for easier comparison. Some level differences can be seen at low and medium frequencies. Below 100 Hz, sequences recorded with guitars Aa and Bb show significantly more bass compared to guitar Cc. The same tendency can be found for guitars Aa' and Bb' compared to Cc' in the second group of guitars without covarying bracewood, as shown in Figure 4. Guitars Cc and Cc' also show a different general curve shape compared to the others between 200 Hz and 500 Hz. For Cc and Cc', the peak at 300 Hz seems to be narrower. Above 1 kHz, all spectra look very similar.

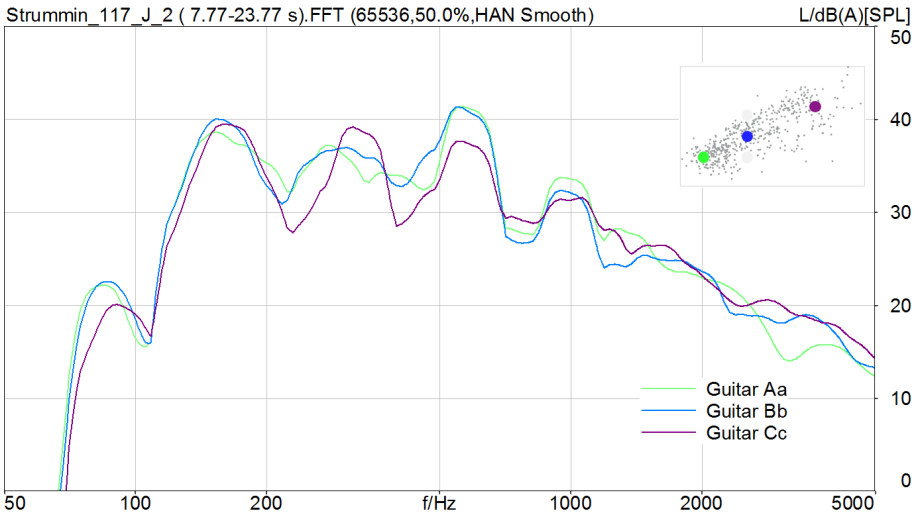

Figure 3 – Averaged spectrum of the strumming sequence for guitars Aa, Bb and Cc.

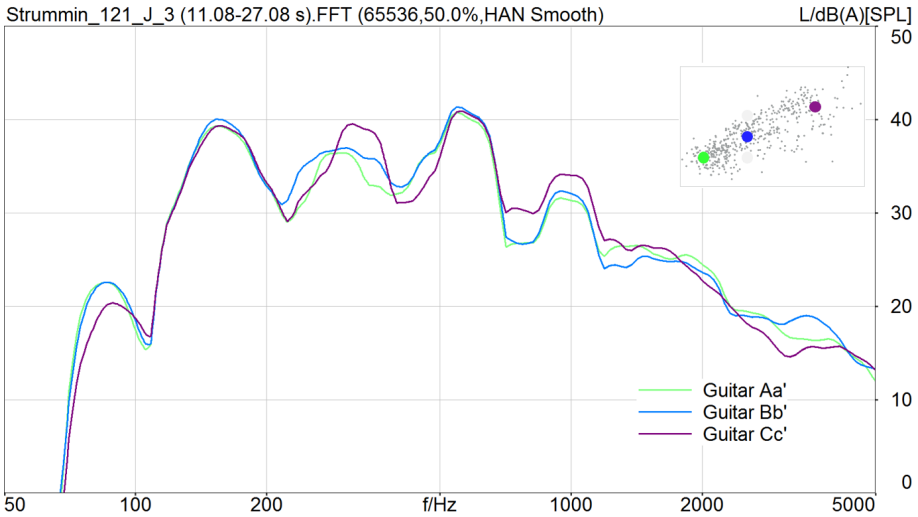

Figure 4 – Averaged spectrum of the strumming sequence for guitars Aa', Bb' and Cc'.

If the guitars with constant density are compared, the differences become smaller. This is in line with smaller preference differences found between these guitars in the listening tests (compare Figure 2). In the first group with covarying soundboard and bracewood, which is shown in Figure 5, an increase in bass level can be seen for guitars with tops of decreasing stiffness. Interestingly, this difference in bass level disappears in the second group shown in Figure 6. No systematic difference at frequencies above 1 kHz is visible.

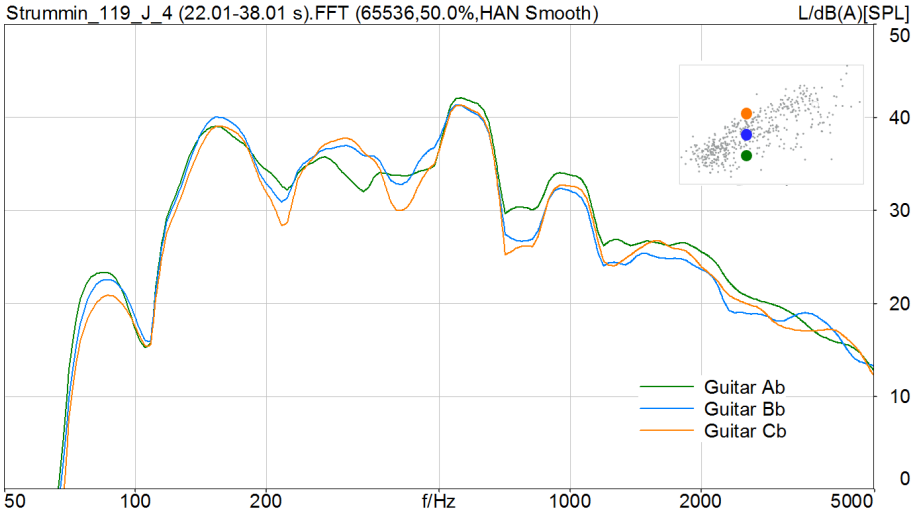

Figure 5 – Averaged spectrum of the strumming sequence for guitars Ab, Bb and Cb.

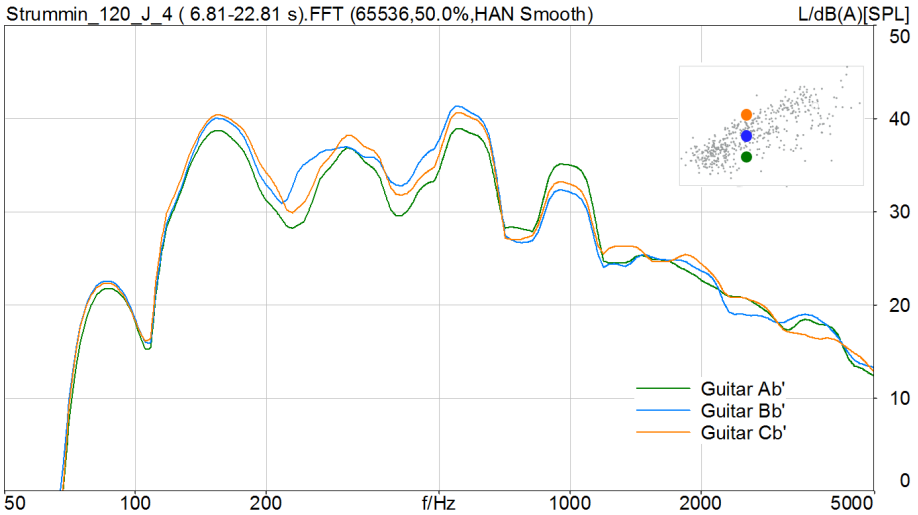

Figure 6 – Averaged spectrum of the strumming sequence for guitars Ab', Bb' and Cb'.

The averaged spectra of the recordings discussed above, of course, depend heavily on the played music sequence. A more detailed analysis is possible if single notes are plucked as will be discussed in Section 5. However, instruments are often characterized by measuring their transfer functions. In this case, the excitation of the guitar body by the strings is replaced with an impact of a hammer on the bridge. The resulting curves show the characteristic resonances of the guitar body. This will be discussed in Section 4. To better understand the vibration behavior of a guitar, a modal analysis has been performed and will be summarized in the following section.

3 Modal analysis

A multiple point modal test was performed using a force impact hammer (B&K 8202 with rubber tip and Dytran 1051 piezoelectric force sensor) and two accelerometers (MMF KS95). The accelerometers had a mass of 2.9 g each, which is small compared to the mass of the soundboard and bracing. The sensors were attached using a thin layer of wax. It was decided to maintain the positions of the accelerometers fixed, as shown in Figure 7 and to rove the hammer between measurement locations. The grid for hammer excitation was marked with paper, which did not add much weight. The strings were retained for the measurement; therefore, no measurement points below the strings between the sound hole and the bridge or at the neck are available. Guitar Aa (114) was chosen for the analysis. The guitar was mounted horizontally on two strips of fabric to avoid strong damping of the back. Additionally, this made it easier to homogeneously strike the guitar from the top keeping the impact angle of the hammer perpendicular to the surface. Each hit was controlled separately to avoid double strokes and to ensure that sufficient energy was introduced in the complete frequency range by monitoring the coherence of the frequency response function.

Figure 7 - Modal analysis with force hammer and two accelerometers. Accelerometers are at fixed positions and the force hammer is used for scanning the surface.

For each impact position of the hammer, a transfer function between force input and acceleration output is calculated. Using the complete dataset, the mode shapes of the soundboard can be calculated. Figure 8 shows snapshots of the maximum deflection for three exemplary modes. Red means outward deflection, blue means inward deflection and green means no movement. Please note that all resonances (top, back and air) are coupled with each other, but only the deflection of the soundboard is visualized here. Missing data points, e.g., at the sound hole, are interpolated for visualization but are not meaningful.

For the $T_{1,1}$ mode (monopole mode) of the top at 156 Hz, strong movement of the outer edges (sides of the guitar) can be seen in Figure 8 (blue). Less movement at the edges is visible for $T_{2,1}$ at 271 Hz (cross dipole mode) and $T_{1,2}$ at 305 Hz (long dipole mode).

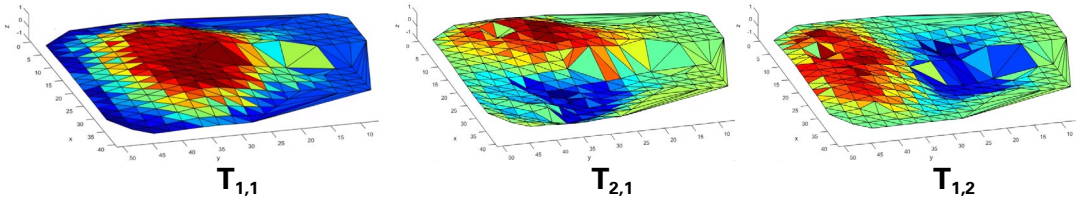

Figure 8 – Snapshot of the measured soundboard deflection for three exemplary modes.

More modes are visualized in Figure 9. At 353 Hz, a deflection similar to the cross dipole can be seen, however, there is stronger movement of the sides. At 501 Hz, the deflection looks similar to a $T_{1,3}$ mode (long tripole) but with small movement near the bridge. The $T_{3,1}$ mode (cross tripole) at 547 Hz and the $T_{4,1}$ (cross quadrupole) at 736 Hz are easier to recognize. Toward higher frequencies, more complex modes can be identified (684 Hz, 785 Hz, 906 Hz, 1032 Hz, etc.) until the measurement grid becomes too coarse.

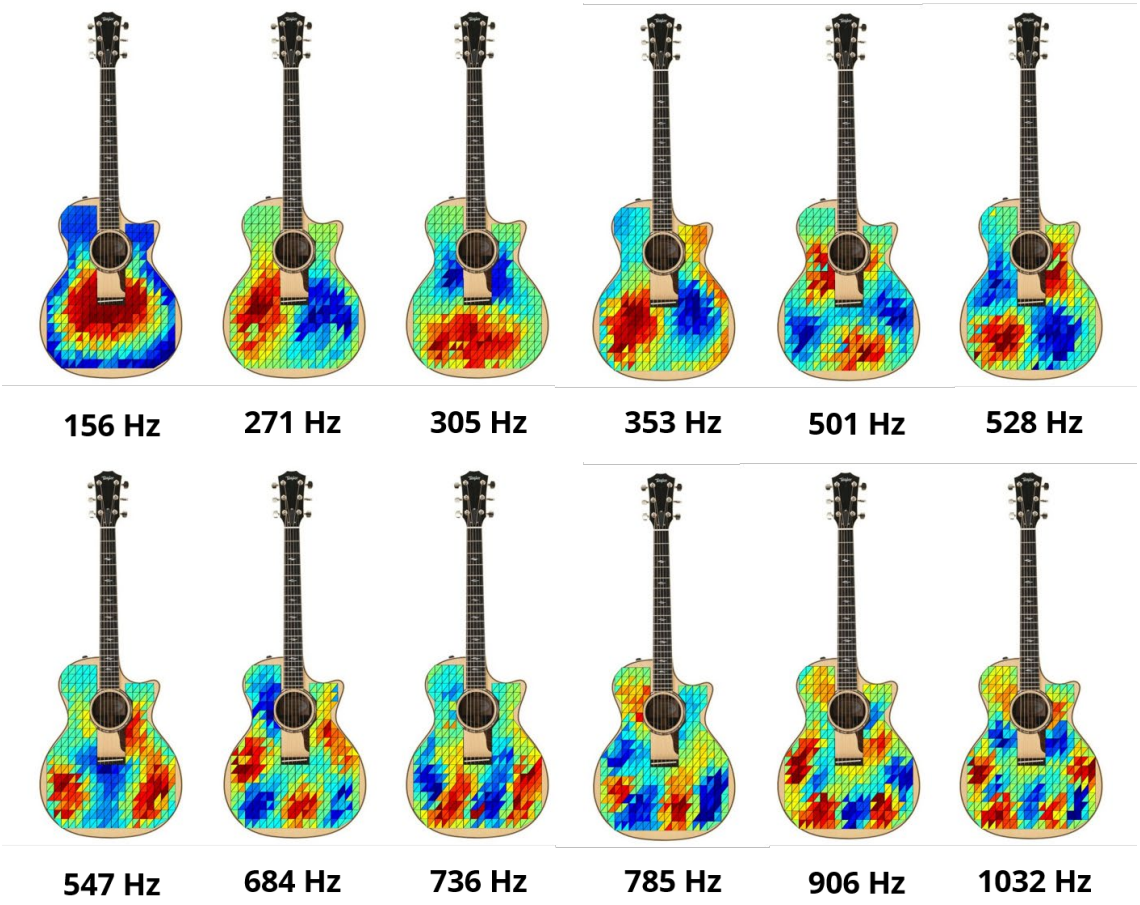

Figure 9 - Measured modal frequencies and corresponding deflection of the soundboard.

We will return to the mode shapes shown here when discussing the sound radiation of the guitars in the following section.

4 Transfer function measurements

The sound radiation of all guitars was measured in the large anechoic chamber at TU Dresden using transfer functions between force excitation of the bridge and sound pressure at three positions. The configuration is shown in Figure 10. The following three measurement microphones were each placed at a 2 m distance: a G.R.A.S. 40HL in *front* of the guitar and two B&K 4188 free-field capsules with B&K 2671 preamplifiers 45° to the *side* and above the guitar (*top*). An accelerometer type MMF KS95 was mounted in the middle of the bridge. All signals were recorded with Head Artemis and a Head Octobox frontend.

Figure 10 – Configuration for transfer function measurements in the anechoic chamber. Marked are the microphones positioned 2 m in front, to the side and above the guitar.

Figure 11 – Excitation of the bridge using an impact hammer with a force sensor.

An impulse hammer B&K 8202 with a rubber tip and a Dytran 1051 force sensor was used to excite the bridge as shown in Figure 11. The photo shows excitation at the "mid" position. "Low" means a hammer impact at the bridge where the low E string is attached. "High" refers to an impact at the high e string. For all transfer function measurements, the strings were damped using the hand, but not (as shown in the picture) in front of the sound hole. The position of the hand was shifted toward the neck to not influence the resonance of the air volume.
Figure 12 shows an exemplary transfer function for all three impact positions. The course of the curves below 240 Hz is nearly identical. At 270 Hz, the general tendency of the curves is inverted for impact at the low and high positions, which will be discussed below. Toward higher frequencies, the amplitudes are somewhat different, but the general shape is similar. Above 640 Hz, large variation can be seen.

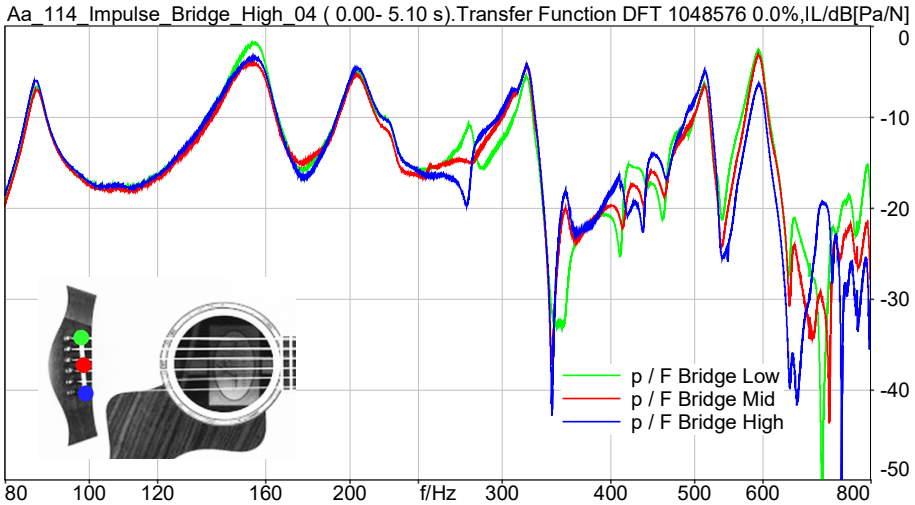

Figure 12 – Transfer function of sound pressure at frontal microphone to force input at bridge for guitar Aa (114) with the back not damped.

In *all* following figures (except where stated otherwise), the average over all three impact positions (low, mid and high) will be plotted for each transfer function. As seen in the averaged transfer function plotted in Figure 13, the variation at 270 Hz nearly disappears. Averaged transfer functions above 640 Hz should be interpreted carefully.
The peaks in the transfer function can now be assigned to the modes determined in Section 3. $T_{1,1}(1)$ is the coupled air resonance of the inner volume, $T_{1,1}(2)$ is the first coupled resonance of the soundboard (top), and $T_{1,1}(3)$ is the first coupled resonance of the back.
$T_{2,1}$ at 270 Hz is radiating much less energy than $T_{1,1}$ because the average deflection of the soundboard is nearly zero. Additionally, $T_{2,1}$ is not excited well if the hammer strikes the bridge in the middle, i.e., exactly on the nodal line. Depending on the excitation on the low or high side of the bridge, the phase angle relative to the neighboring modes changes for $T_{2,1}$ and explains the different course of the transfer function that had already been noticed in Figure 12.
The peak above 300 Hz can be assigned to the $T_{1,2}$ mode. Good sound radiation can be observed in the figure, maybe because the mode becomes asymmetric due to the sound hole and the tapering of the guitar body.
The two dominant peaks between 500 Hz and 600 Hz are again modes with nonzero average deflection: $T_{1,3}$ and $T_{3,1}$. The strong dip between them can be explained by cancellation effects because of the antiphase of the radiated sound from both modes in

that area. The mode $T_{2,2}$ also has a frequency in the 500 Hz area, but its effect is probably neglectable because of its expected small total volume velocity.

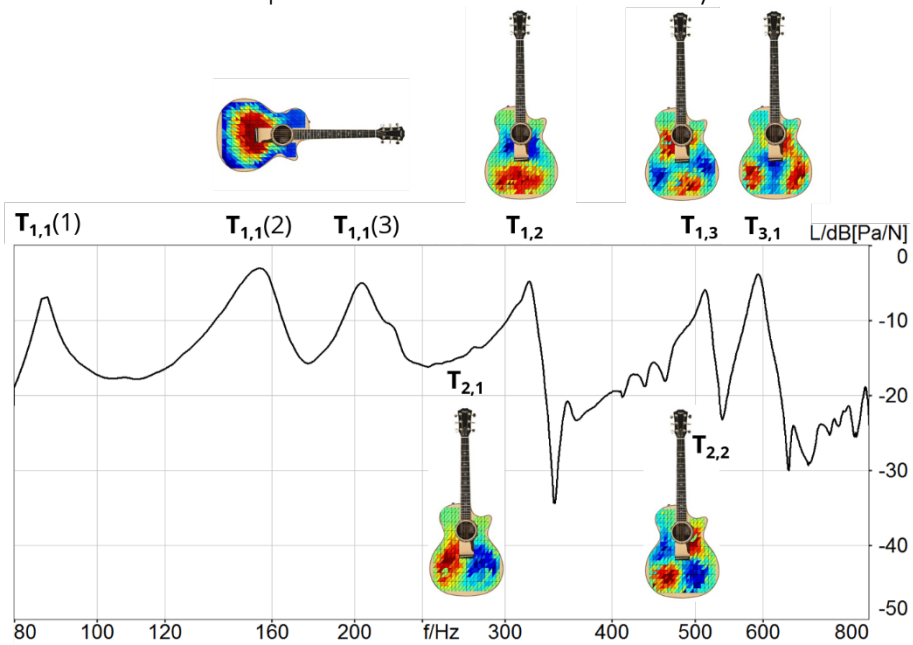

Figure 13 – Transfer function of frontal microphone to force input at bridge for guitar Aa (114) averaged over all three impact positions at the bridge. Additionally, dominant modes are assigned to the peaks.

Between 340 Hz and 500 Hz, several peaks and dips are observable in Figure 13 that cannot be assigned to modes of the soundboard. Interestingly, these resonances are reduced if the back of the guitar is damped by pressing it against a bale of fabric. Figure 14 shows corresponding measurements individually for the hammer strikes at bridge positions low, mid and high.

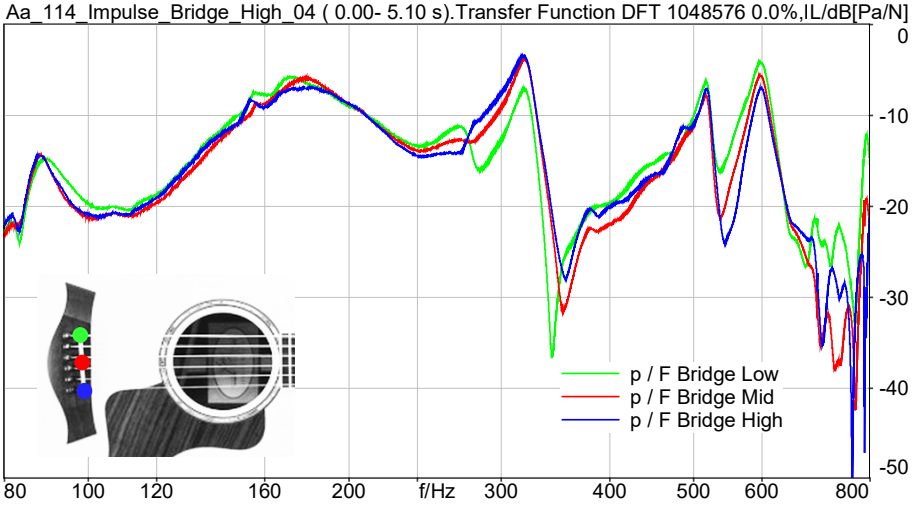

Figure 14 – Transfer function of sound pressure at frontal microphone to force input at bridge for guitar Aa (114) with the back damped by pressing it against a bale of fabric.

A direct comparison of guitar Aa with a damped and undamped back using averaging over all three impact positions for each curve is plotted in Figure 15. In addition to the smoothing of the frequency response between 340 Hz and 500 Hz, the missing back resonance $T_{1,1}(3)$ and a frequency shift and damping of the top resonance $T_{1,1}(2)$ is

observable. Additionally, the coupled air resonance $T_{1,1}(1)$ is reduced in level. No strong influence on higher top modes ($T_{1,2}$, $T_{1,3}$ and $T_{3,1}$) can be seen by damping the back of the guitar.

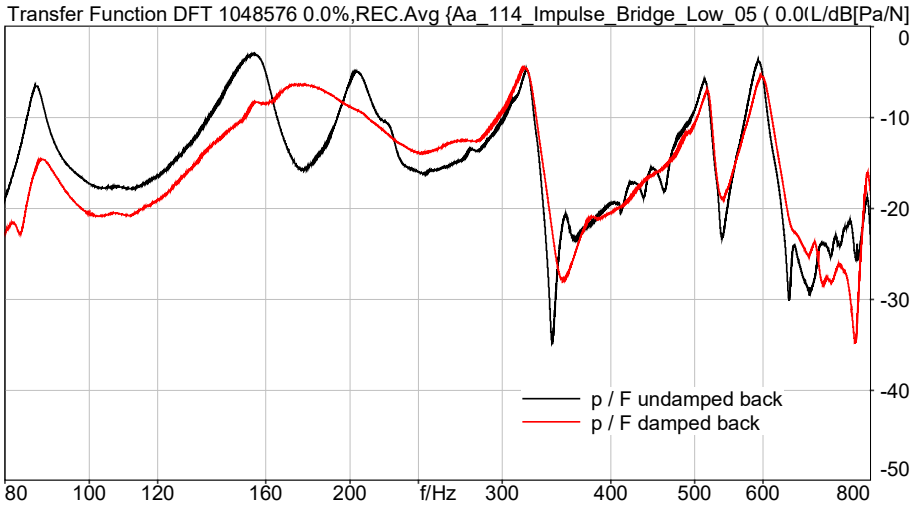

Figure 15 – Transfer function of frontal microphone to force input at bridge for guitar Aa (114) averaged over all three impact positions at the bridge.

If a guitar is played by a musician, the real damping of the back might be something between the two cases discussed above. *For this study, it was decided not to dampen the back of the guitars for the following comparisons.*
In some publications, the sound pressure level or a normalized plot of the same is used to characterize guitars by tap testing. For comparison, the transfer function (*p*/*F*) discussed so far is plotted versus the measured sound pressure level in Figure 16.

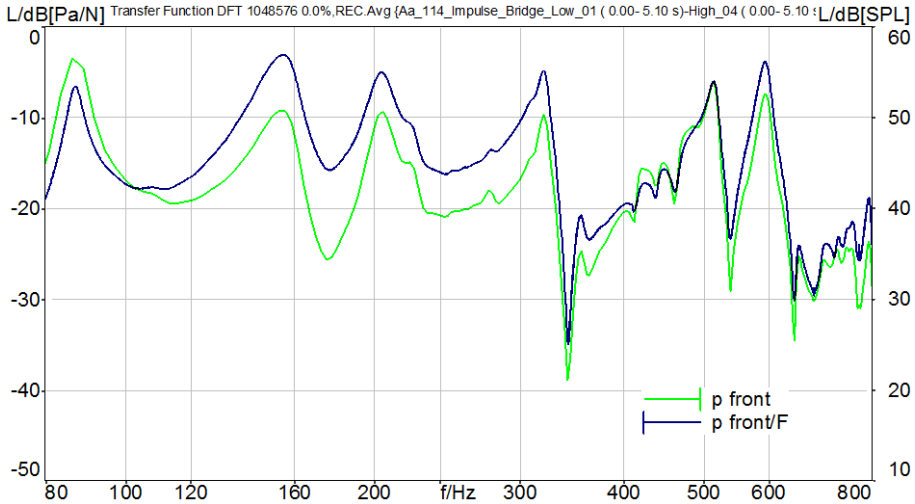

Figure 16 – Comparison of the transfer function of sound pressure *p* at the frontal microphone to force input *F* at the bridge versus sound pressure level only.

The difference between *p* and *p*/*F* is basically a simple frequency weighting. Both would be good for discussion. However, the transfer function *p*/*F* will be used because the normalization to the input strength simplifies the measurements and eases the comparison (especially of the amplitude) between different instruments.

A comparison between the three microphone positions is plotted in Figure 17. The transfer function toward the frontal (red) and side (blue) microphone positions is quite

similar, except in the region near 300 Hz. The dominant mode in this frequency range, $T_{1,2}$, seems to radiate well toward the front but shows some cancellation effects toward 45° to the side. Much more deviation can be seen at the top (green) microphone position, i.e., the direction of the head of the musician. Interestingly, the overall level at frequencies below 200 Hz is lower than the front or side, suggesting that the guitar is not radiating as an omnidirectional monopole at those low frequencies where the modes $T_{1,1}(1)$ and $T_{1,1}(2)$ are dominating. The level at 200 Hz, where the back resonance $T_{1,1}(3)$ is active, is comparable in all directions. However, the head of a musician is not 2 m away from the sound hole. If the aim is to compare the acoustic impression of the player with the sound that a listener is hearing in front of the guitar, the green curve should be increased in level to compensate for the smaller distance. Additionally, the body of a guitarist influences the radiation from the back of the guitar. In the measurements, the experimenter was standing behind the guitar, but somewhat to the side, as shown in Figure 11. Therefore, conclusions should be drawn carefully.

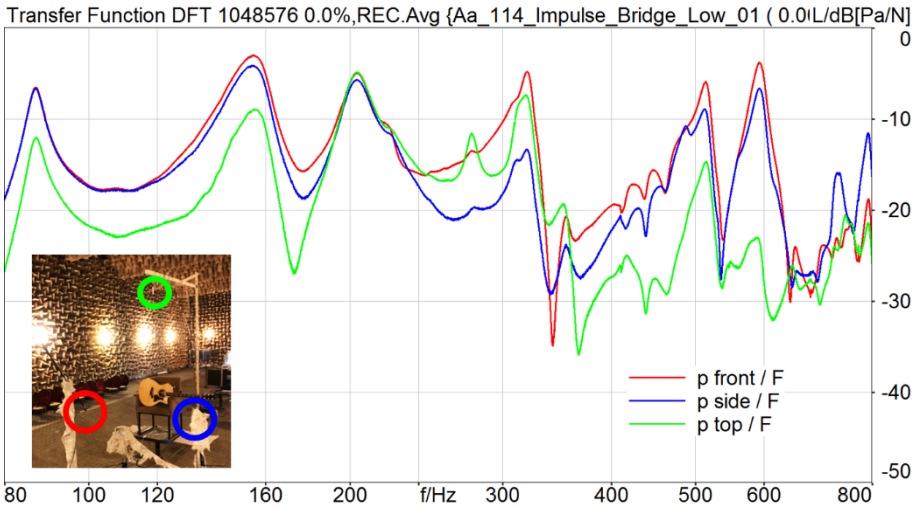

Figure 17 – Transfer functions of sound pressures at front versus side versus top microphone to force input at bridge for guitar Aa (114).

The good sound radiation of mode $T_{2,1}$ at 270 Hz toward the top is also noticeable. At frequencies above 340 Hz, the directivity of the guitar increases with better radiation in the horizontal plane. *Because only the recording of the frontal microphone was used in the listening tests, all future comparisons are plotted for the frontal direction only.*

After discussing the general vibroacoustic behavior of a guitar and motivating the measurement decisions, we can now compare different guitars with varying material properties. Three guitars from the first group built with covarying soundboards and bracewood with a similar ratio of longitudinal Young's modulus and density are selected. This constant ratio means that the speed of sound in the longitudinal direction is also comparable. Therefore, the guitars were labeled "constant c". It was expected that this constant ratio would result in equal modal resonance frequencies. However, in Figure 18, the resonances in the transfer functions are not equal but a systematic increase from Aa to Cc can be observed.
It was already discussed in part 2 of this report that this increase could be explained by the influence of the heavily varying shear modulus of the selected soundboards.
By varying the material properties of the top, the top modes (e.g., $T_{1,1}(2)$) are shifted in frequency, and a similar influence on the coupled first back mode $T_{1,1}(3)$ and even the coupled air mode $T_{1,1}(1)$ is visible. This shift of the modal frequencies can explain some

of the variations found in the recorded music sequence analyzed in Section 2. For example, the lower resonances of guitars Aa and Bb result in more bass.
It was expected that heavier soundboards would result in a generally lower level. However, no systematic influence of increasing mass on overall level can be seen in Figure 18, which is also true for higher frequencies above 800 Hz plotted in the Appendix in Figure 38 and Figure 39. This is in line with the small loudness differences found in the music recordings.

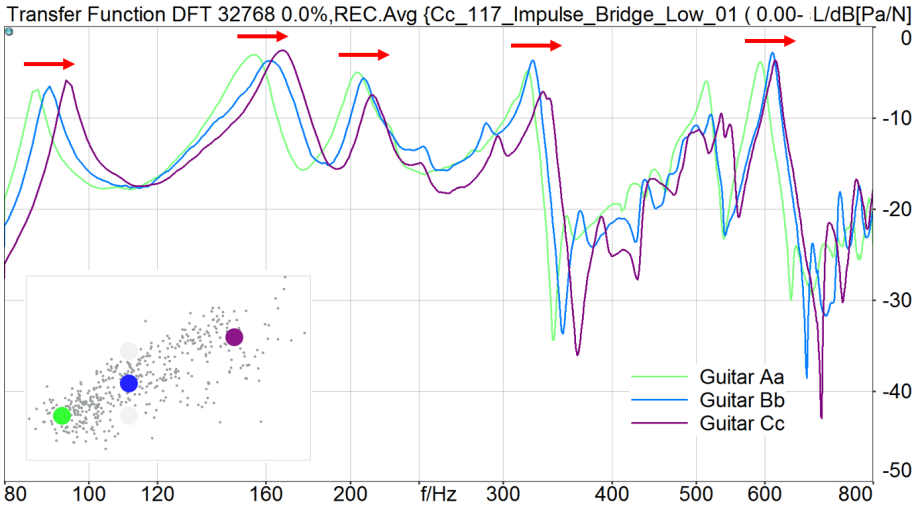

Figure 18 - Comparison of guitars Aa, Bb and Cc (const. c) using the transfer function of the frontal microphone to the force input at the bridge.

Similar behavior with the same tendencies can be observed in the second group of guitars shown in Figure 19. These guitars were built with varying soundboard properties but the bracewood was held constant at medium values. This could explain why the frequency shifting is smaller than that in the first group. The similar trend in the frequency shift supports the hypothesis that this variation is not a result of manufacturing tolerances.

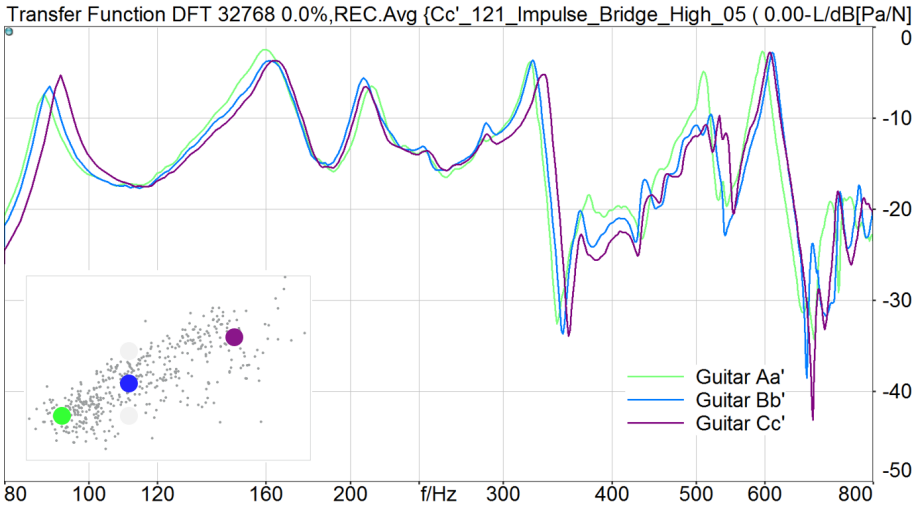

Figure 19 - Comparison of guitars Aa', Bb' and Cc' (const. c) using the transfer function of the frontal microphone to the force input at the bridge.

Small changes in resonance frequencies are also observed if the mass of the tops (soundboards and bracewood) is held constant and only the stiffness is varied. This can be seen by comparing guitars Ab, Bb and Cb in Figure 20. Again, the varying bass in the corresponding recorded music sequences is shown in Figure 5. Increasing the stiffness from guitar Ab (green) to guitar Bb (blue) increases several coupled resonance frequencies (e.g., $T_{1,1}(1)$, $T_{1,1}(2)$, $T_{1,2}$, …), but not all frequencies (e.g., $T_{1,1}(3)$). Surprisingly, there is not much difference in the resonance frequencies between guitars Bb (blue) and Cb (orange), except for $T_{1,1}(3)$.

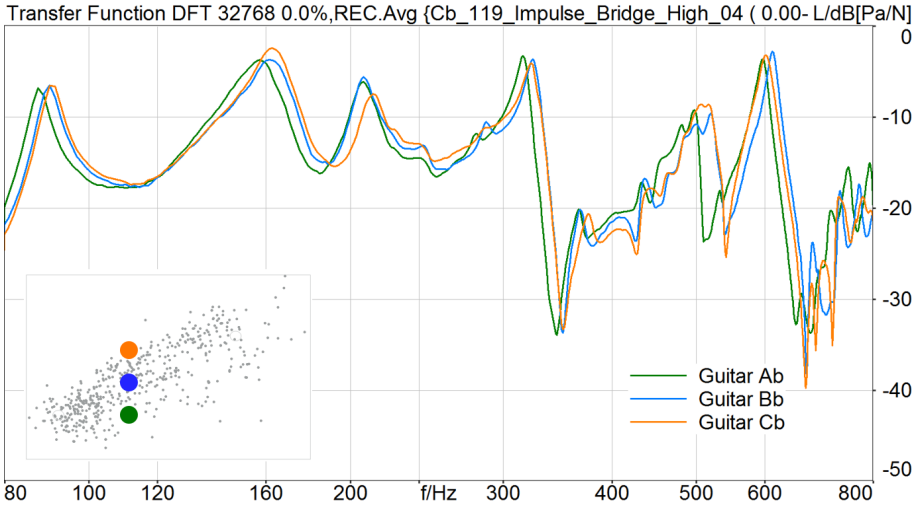

Figure 20 - Comparison of guitars Ab, Bb and Cb (const. m) using the transfer function of the frontal microphone to the force input at the bridge.

Even more astonishing, in the second group of guitars, which were built with constant bracewood parameters, there is no resonance shift for increasing stiffness (see Figure 21). Consistent is the observation that the corresponding recorded music sequences shown in Figure 6 show less variation regarding their spectra, especially for bass frequencies below 100 Hz.

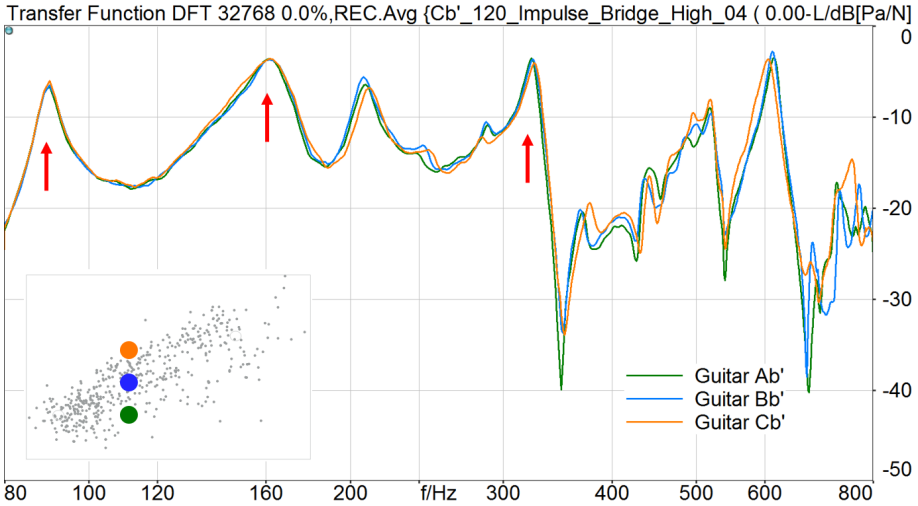

Figure 21 - Comparison of guitars Ab', Bb' and Cb' (const. m) using the transfer function of the frontal microphone to the force input at the bridge.

Thus far, guitars with varying soundboards (or varying soundboards and covarying bracewood) have been compared. To discuss the influence of the bracewood material parameters on the vibroacoustic behavior, guitars with the same soundboard but varying bracewood are plotted pairwise in Figure 22. For example, for guitars Aa and Aa' in the top left graph, the soundboards have the same material properties (low stiffness and low density). However, the bracewood of Aa' is held at median values, while the bracewood of Aa has lower density and stiffness. The reduced overall stiffness of Aa compared to Aa' pulls the resonances toward lower frequencies. The reduced mass pushes the resonances toward higher frequencies. The measured frequency shift in the top left graph of Figure 22 suggests that the stiffness effect wins. Decreasing stiffness alone in the top right graph (Ab' → Ab) should reduce the resonance frequencies, which is also visible. Increasing stiffness alone in the bottom left graph (Cb' → Cb) should increase resonance frequencies, which is not visible. Finally, in the bottom right graph, decreasing mass should lower resonances, but increasing stiffness pulls toward higher resonance frequencies (Cc' → Cc). Again, the measured frequency shift suggests that the stiffness effect wins.

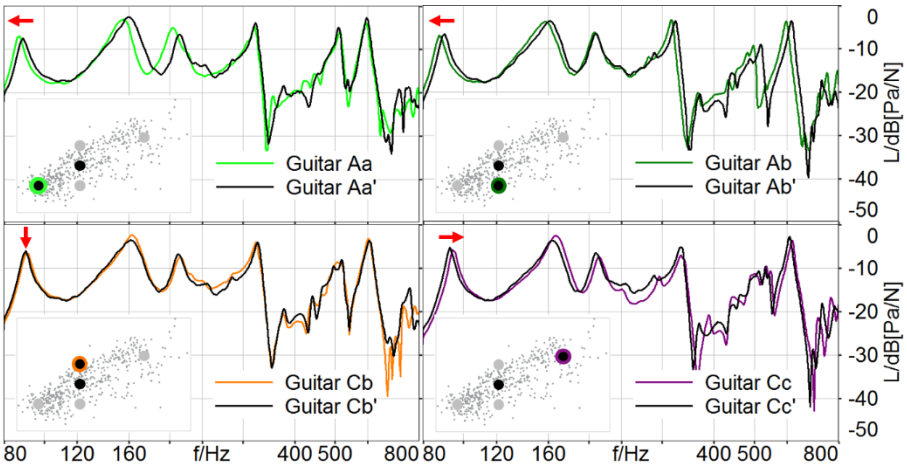

Figure 22 - Pairwise comparison of guitars from groups 1 and 2 using the transfer function of the frontal microphone to the force input at the bridge. In each pair, only the bracewood material parameters vary. The expected shifts of the resonance frequencies are as follows:

- **top left: Aa' → Aa decreasing stiffness (shift to left), decreas. mass (shift to right)**
- **top right: Ab' → Ab decreasing stiffness (shift to left)**
- **bottom left: Cb' → Cb increasing stiffness (shift to right; not visible)**
- **bottom right: Cc' → Cc increas. stiffness (shift to right), increas. mass (shift to left)**
- **Bb = Bb' and is therefore not plotted here**

The observed resonance shifts are not always coherent with the expected shifts. This discrepancy could be because of manufacturing tolerance or because the effect of the shear modulus, which was not controlled here, might not be negligible.

In summary, the measurements confirm that there is a strong influence of the natural variation of wood material properties on the guitar resonances. Specifically, the varying bass intensity in the music recordings can be linked to the resulting resonance shifts. Surprisingly, no influence of top density on the level of the transfer functions and the resulting loudness of the recordings was found.

The shift in the resonance frequencies measured in the transfer functions above and the resulting balance between bass and higher frequencies in the played music pieces is probably one dominant reason for the preference ranking in the listening tests. However, even for guitars with nearly identical transfer functions (e.g., Ab', Bb' and Cb') a (nonsignificant) preference tendency was found (compare Figure 2). This supports the hypothesis that there must be at least one additional attribute in the sound of the guitar that influenced the preference.

Thus far, the guitar body has been discussed as a separate resonance system. However, the body is coupled and therefore interacts with the strings. The fundamental range of the strings, the corresponding scale notes and an exemplary transfer function are shown in Figure 23.

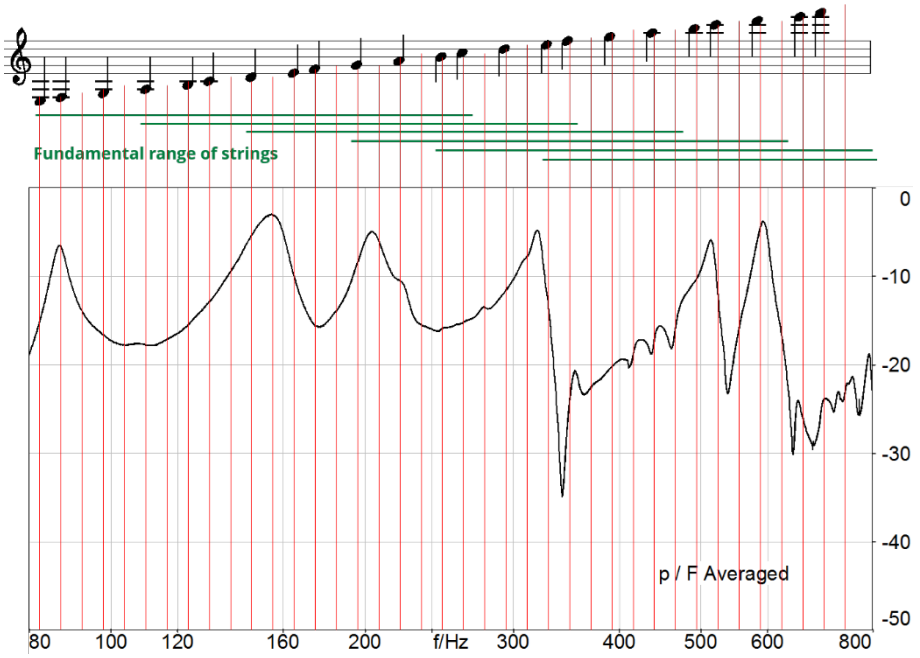

Figure 23 – Comparison of scale notes with the transfer function of guitar Aa.

5 Plugged single notes

To investigate the interaction between strings and body, plugged tones were recorded in the anechoic chamber using the same configuration as for the transfer function measurements. A helper tool was made using spring steel wrapped in an insulating hose. The strings were plugged in front of the sound hole as shown in Figure 24, which resulted in a uniform excitation of approximately 1 N plugging force in the vertical direction.

Figure 24 – Manual plugging of single notes using a helper tool made of spring steel wrapped in an insulating hose.

Plugged tones were recorded for all strings stopped at all frets up to the 12th fret. Figure 25 shows the overlaid spectrum of all tones of the low E string measured at the frontal microphone position. To better be able to compare it with the transfer function of the corresponding guitar, no A-weighting was applied to the spectrum. For each tone, the fundamental and several harmonics can be seen, which are plotted in the same color.

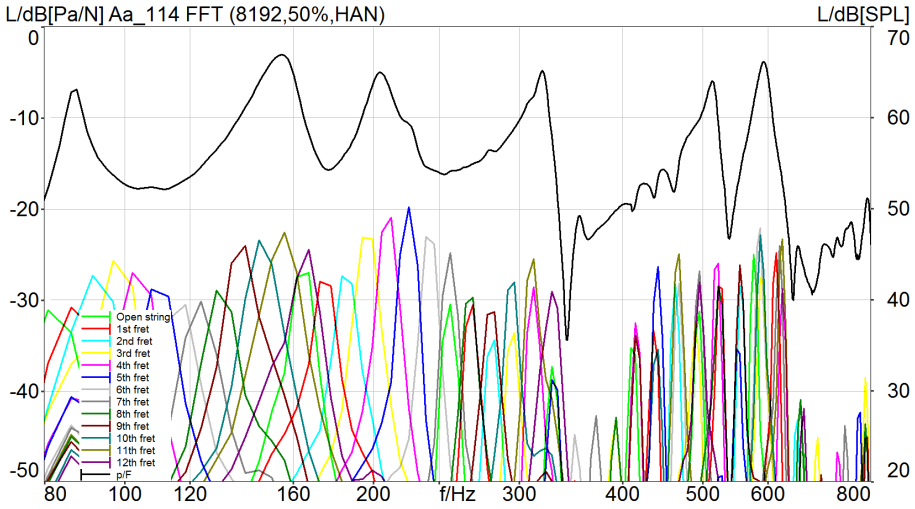

Figure 25 – Overlaid spectrum of 13 tones (low E string, open to the 12th fret) recorded at the frontal microphone position. For comparison, the transfer function of the corresponding guitar Aa is shown.

Despite the manual plugging of the strings, the envelope of the overlaid tone spectra is very similar to the shape of the transfer function. This means that the loudness of each partial is directly influenced by the coupled air and body resonances of the guitar. This also seems true for frequencies above 800 Hz as seen in Figure 26. For better comparison, the 1/24th octave smoothed sum of all tones (dashed) and the smoothed transfer function (black) are shown. Toward the higher frequencies, the distance between these two curves increases, maybe because less energy is transferred from the string to the guitar body. Above approximately 2000 Hz, the peaks and dips no longer seem to coincide.

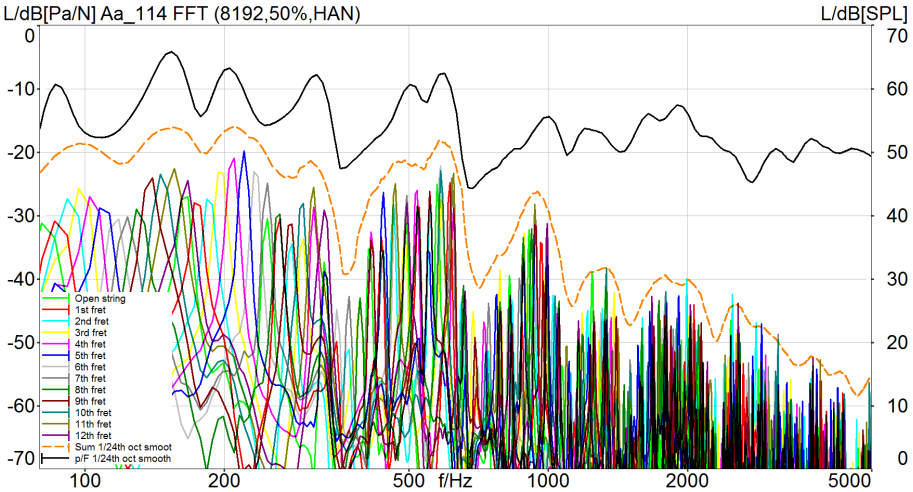

Figure 26 – Overlaid spectrum of 13 tones (low E string, open to the 12th fret). For better comparison, the 1/24th octave smoothed sum of all tones (dashed) and the smoothed transfer function of the corresponding guitar Aa are shown.

Additionally, for other strings, the loudness of the partials is connected with the shape of the transfer function. However, a roll-off in level can be observed below 220 Hz toward lower frequencies for string a (Figure 27, left) and string d (Figure 27, right).

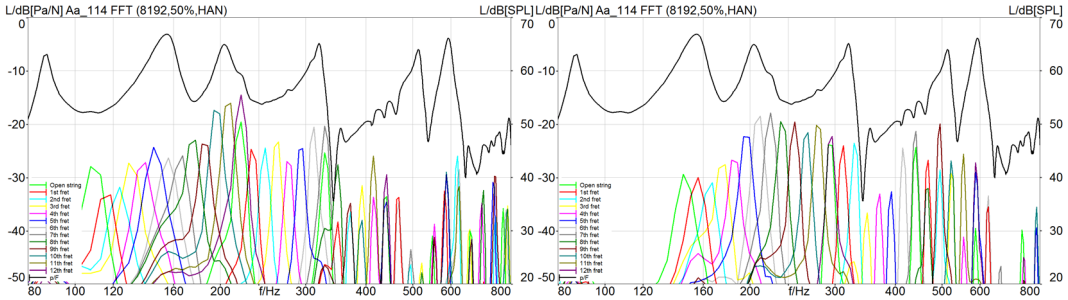

Figure 27 – Overlaid spectrum of 13 tones for the a string (left) and d string (right). For comparison, the transfer function of the corresponding guitar Aa is shown.

A similar roll-off was found for string g below 300 Hz, as plotted in Figure 28. Interestingly, the influence of the transfer function on tone level is no longer that strong. Remaining prominent is the decrease in level above 600 Hz, but the overall envelope of partial levels does not seem to follow the transfer function well. It will be shown later, using the example of the g string, that the resonances of the guitar body heavily influence the temporal behavior of the partials. However, the strong correlation between transfer function and overall level of the partials seems to be reduced toward the higher strings.

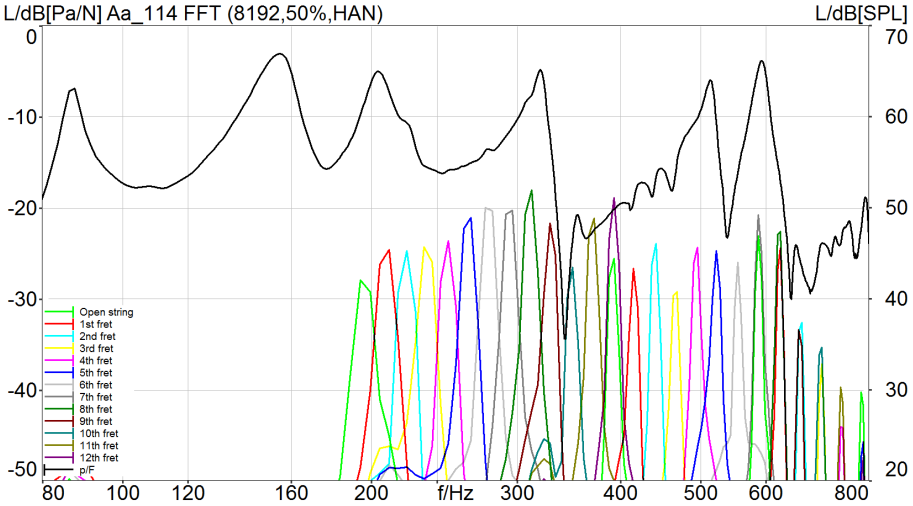

Figure 28 – Overlaid spectrum of tones for the g string and transfer function of guitar Aa.

The same plugged tones as in Figure 28 are plotted again for a wider frequency range in Figure 29. Again, a smoothed sum of all recordings (orange) and the smoothed transfer function (black) are plotted. In comparison with the E string (Figure 26), much fewer similarities can be found between the two curves.

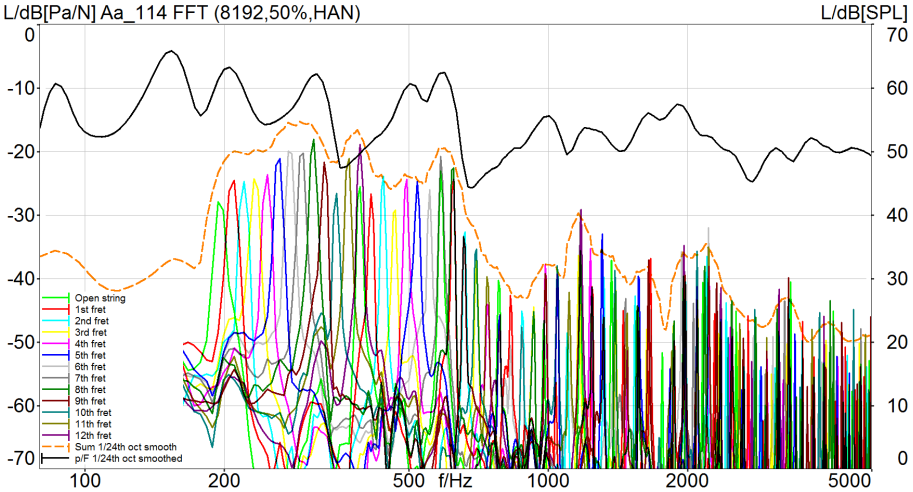

Figure 29 – Overlaid spectrum of 13 tones (g string, open to the 12th fret). For better comparison, the 1/24th octave smoothed sum of all tones (dashed) and the smoothed transfer function of the corresponding guitar Aa are shown.

Figure 30 confirms the tendency of reduced influence of the transfer function on the level of the partials for the two highest strings (b and high e).

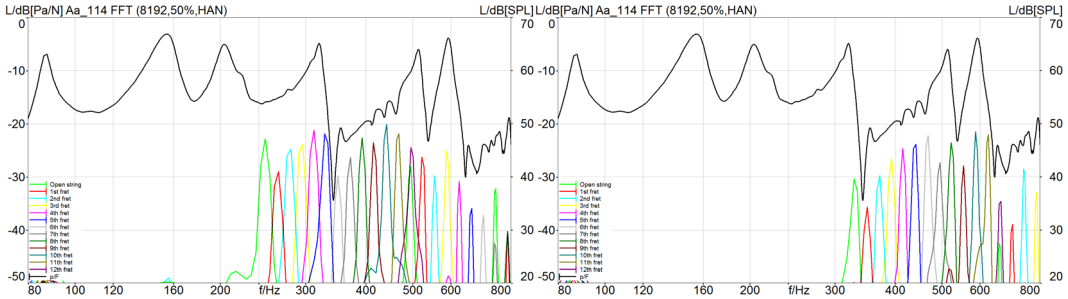

Figure 30 – Overlaid spectrum of 13 tones for the b string (left) and high e string (right). For comparison, the transfer function of the corresponding guitar Aa is shown.

The overall loudness of a plugged tone is influenced by the sum of its fundamental and all of its harmonics, considering the perceptual characteristics of our hearing apparatus, e.g., decreasing sensitivity toward lower frequencies or masking at higher frequencies. Figure 31 shows the separately calculated loudness of 65 plugged tones of guitar Aa. A perceptual modal after ISO 532 B was used for calculation. Only small variation in loudness between the individual notes can be seen. This means that the overall loudness of a tone does not correlate with the transfer function, because the varying loudness effects of multiple partials seem to compensate for each other.

If all loudness versus time plots of all recorded plugged tones are averaged for a single guitar, the average loudness of that guitar can be calculated. For guitar Aa, the maximum value of this averaged loudness is 12.9 sone. For guitar Cc, the same averaged loudness value of 12.9 sone was calculated. This confirms the neglectable loudness differences between the guitars, which were previously discussed using the recorded music sequences and measured transfer functions, despite the differences in the weight of the soundboards.

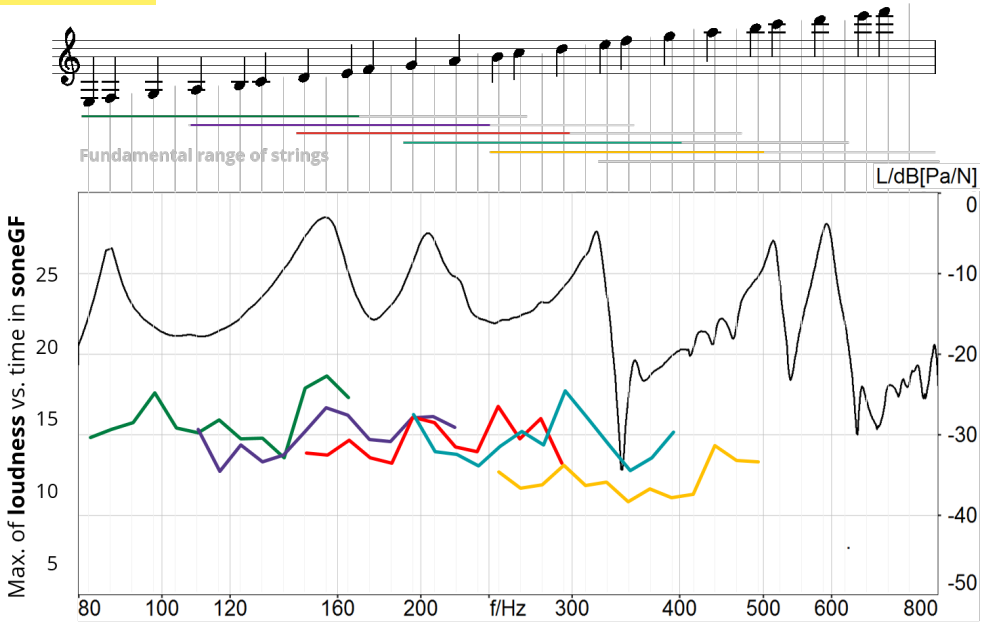

Figure 31 – Maximum loudness versus time calculated after ISO 532 B of 13 plugged tones for each string E, a, d, g and b. For comparison, the transfer function of the corresponding guitar Aa is shown.

Thus far, the loudness of plugged tones and their partials in relation to the measured transfer functions was discussed. However, the resonances of the guitar body also influence the temporal behavior. This is illustrated exemplarily for tones of the g string in Figure 32. If a partial is close to a resonance, the vibration energy of the string is quickly transferred to the guitar body and radiated as sound. Therefore, the decay of this partial is short compared to a partial that is further in frequency from the body resonances. However, the overall level of these partials can still be the same (compare Figure 28). The varying decay of partials can be seen well for the fundamentals of the tones in Figure 32. The lowest tone is g. Its fundamental at 196 Hz lies below the $T_{1,1}(3)$ coupled back resonance at 204 Hz and shows a long decay. The fundamental of the next scale note g# (208 Hz) coincides more with $T_{1,1}(3)$ and has, therefore, a dramatically short decay. Toward higher tones (a, b♭, b and c), the frequency difference between fundamental and body resonance increases and the decay becomes longer. Following

the scale further (c#, d and d#), the fundamental becomes closer to the next sound radiating resonance $T_{1,2}$ at approximately 320 Hz. Consequently, the decay length decreases again. $T_{1,2}$ lies directly between tone d# (311 Hz) and e (330 Hz) and both are affected nearly equally. For further increasing tone pitch (e, f and f#), an again growing decay of the fundamental can be seen as expected.

Sometimes, amplitude modulation can be observed if a partial is near a resonance (e.g., the fundamental of note a or the first harmonic of note c). The cross-dipole mode $T_{2,1}$ at 271 Hz between the fundamentals of c and c#, which is not radiating much sound, also does not seem to influence the decay or cause amplitude modulation.

The same influence of distance between the frequency of a partial and the frequency of a body resonance on decay length can be observed for the first harmonics. Long decay can be seen for the first harmonic of g, g# and a. As the partial frequency becomes closer to the next body resonance at approximately 513 Hz, the decay becomes shorter (b♭, b and c). The first harmonic frequency of the tone c# lies directly between the $T_{1,3}$ and $T_{3,1}$ peaks of the transfer function and decays slightly longer; however, for tone d, the frequencies coincide again and a shorter decay is visible.

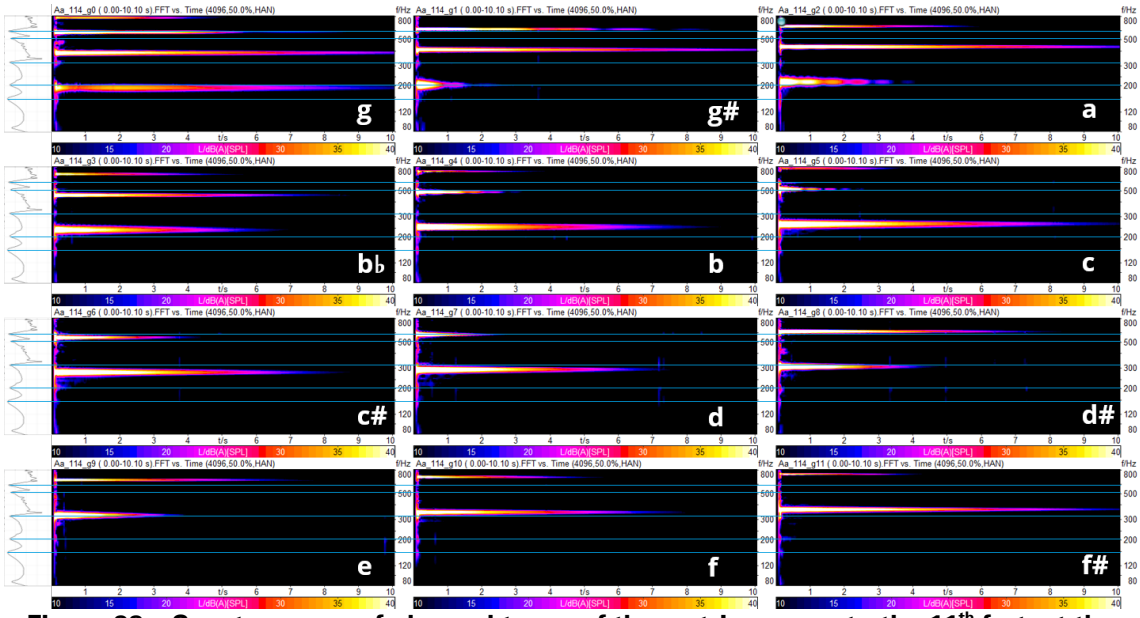

Figure 32 – Spectrograms of plugged tones of the g string, open to the 11th fret, at the microphone positioned 2 m in front of the sound hole of guitar Aa. For comparison, the corresponding measured transfer functions are plotted on the left. Dominant resonance frequencies are marked with blue lines.

Perhaps this frequency dependent decay of partials does influence the quality of the guitar tone. Therefore, an attempt was made to visualize the data in a more compact form. Figure 33 shows the *averaged* spectrogram of *all plugged tones from string g*. Again, the corresponding transfer function is plotted for comparison on the left and dominant resonance frequencies are marked with blue lines. The short decay of partials can be seen clearly for $T_{1,2}$ at approximately 320 Hz and $T_{1,3}$ at approximately 513 Hz. Both modal frequencies lie nearly exactly between two scale notes (compare Figure 23). However, several neighboring tones seem to be influenced in both cases. Surprisingly, the resonance at approximately 593 Hz does not seem to heavily influence the average decay in its neighborhood. This is even more surprising because its frequency is very close to a scale tone (tone d5 with 587 Hz). Nevertheless, an influence of nearby modal

frequencies on the decay of partials could be confirmed in several cases. Therefore, a coarse tuning of modal resonances in the guitar design process seems plausible to avoid multiple harmonics of a single tone decaying too quickly.

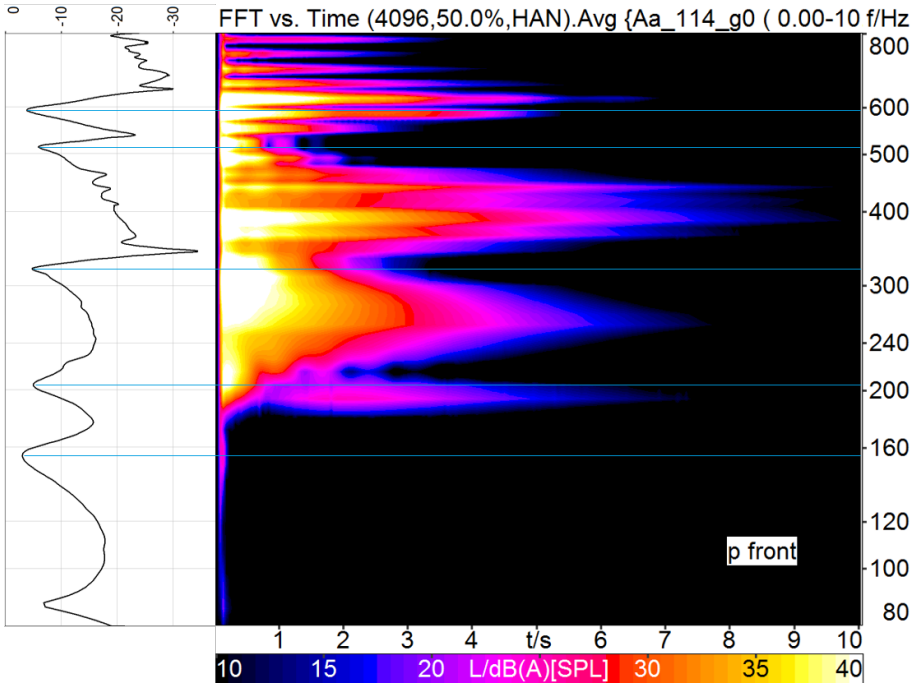

Figure 33 – Averaged spectrogram of 13 plugged tones (guitar Aa, g string, open to the 12th fret). For comparison, the measured transfer function is shown.

Next, all 78 plugged tones of guitar Aa were averaged to include the effect of all strings and a wider frequency range. The resulting spectrogram is shown in Figure 34.

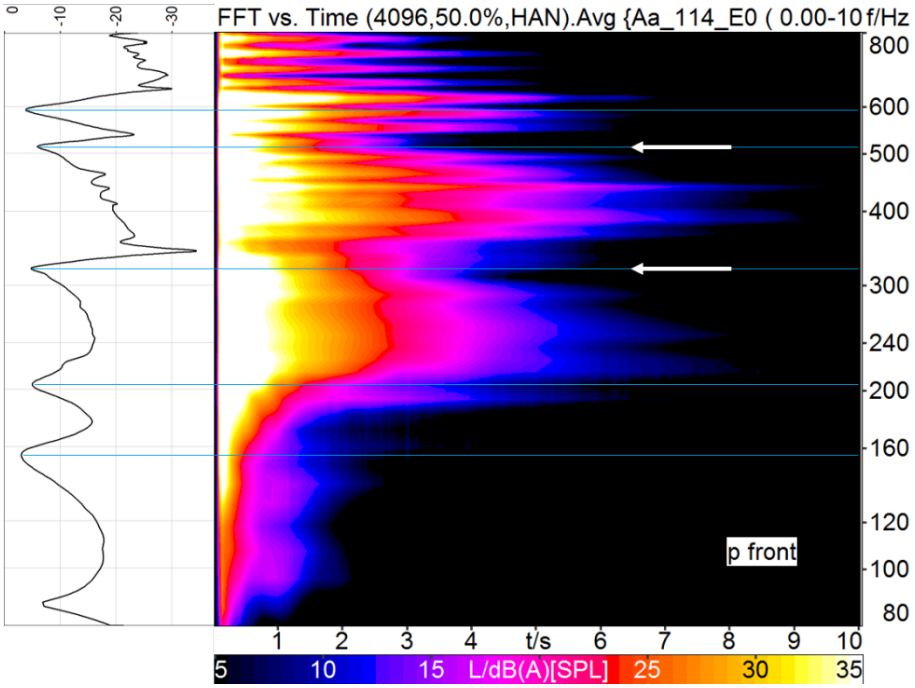

Figure 34 – Averaged spectrogram of 78 plugged tones (guitar Aa, all strings, open to the 12th fret). For comparison, the measured transfer function is shown.

The short decay of partials for the two resonances discussed above at approximately 320 Hz and 513 Hz can still be seen in Figure 34. The decay at lower frequencies does not seem to be heavily influenced by the three coupled $T_{1,1}$ modes. Some influence of these low frequency modes can be seen when analyzing the individual plugged notes (compare Figure 40 to Figure 45 in the Appendix). However, most partials below 200 Hz decay quickly compared to higher harmonics, and for the average shown in Figure 34, the influence of the modal resonances on the decay is nearly invisible.

For comparison, the averaged spectrogram of all plugged tones is plotted for guitar Cc in Figure 35. For this guitar, in comparison to guitar Aa, the modal resonances are shifted toward higher frequencies (see Figure 18). A different decay behavior can be seen for guitar Cc compared to guitar Aa. In addition to the fast decay at approximately 540 Hz, the partial near the 616 Hz resonance decays quickly as well. However, no special influence can be seen at the resonance of approximately 335 Hz.

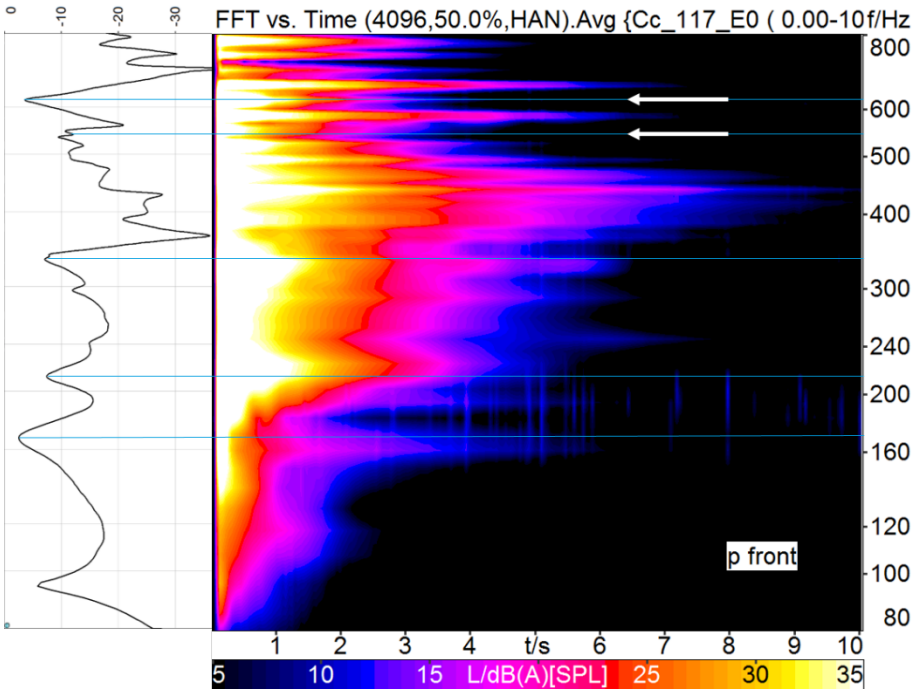

Figure 35 – Averaged spectrogram of 78 plugged tones (guitar Cc, all strings, open to the 12th fret). For comparison, the measured transfer function is shown.

The overall duration of a tone is determined by the sum of its partials. This overall duration will be characterized in the following with a single value for better comparison of decay between individual plugged tones. Therefore, the A-weighted sound pressure level of each plugged tone is plotted versus time. Figure 36 shows an example of the note a# (a string stopped at the 1st fret, guitar Aa, fundamental at 116.5 Hz). A linear regression curve is fitted to a level drop of 15 dB in the initial part of the decay (-5 dB to -20 dB below the maximum). A tone duration T15 is defined, which corresponds to the estimated time needed for a 60 dB decay using this fitted curve. In the example, a tone duration of approximately 10 s is calculated.

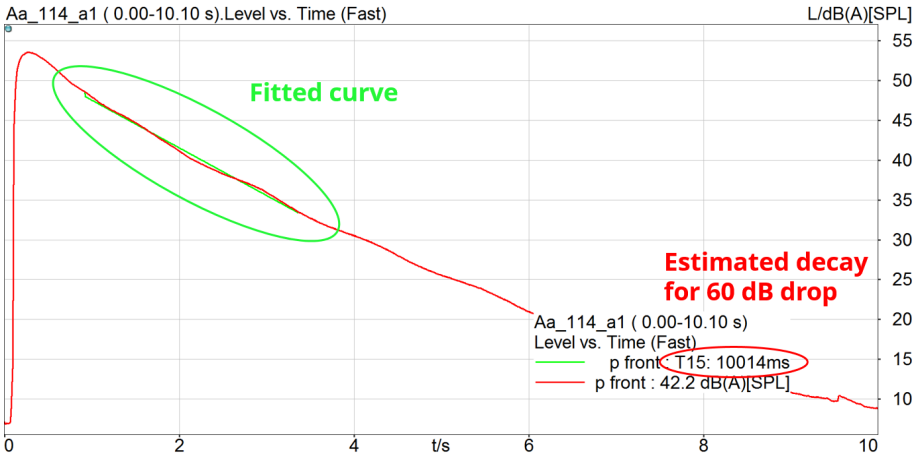

Figure 36 – Level versus time plot for plugged tone a# (a string, 1st fret). A regression line is fitted to the decaying level from -5 dB to -20 dB below the maximum. The tone duration T15 corresponds to the estimated time needed for 60 dB decay using this regression.

The same method can also be applied to calculate the decay of band-passed individual partials. Unfortunately, amplitude modulation often complicates the curve fitting and meaningful results can only be obtained for some partials. The method is better suited for unfiltered tones, where the influence of modulation of individual partials is small. Figure 37 shows the calculated tone durations T15 for 65 plugged tones of guitar Aa. The colors represent the corresponding strings (low E, a, d, g and b). The tones recorded with the b and high e string show much amplitude modulation (see Figure 45 in the Appendix). T15 for the high e string is therefore not included in Figure 37. As expected, the tone duration shows some variation between notes but is not following the transfer function. Maybe a guitar with less harmonics (e.g., a classical guitar with nylon strings) could show a different behavior. Striking is the long duration of plugged tones from several open strings. The highest values can be seen for the open d and g strings. Additionally, for the g string (dark green), the notes g# and a have a long duration. This can be explained by the slow decay of the corresponding first harmonics at 415 Hz and 440 Hz, which are far from the neighboring body resonance frequencies (320 Hz and 513 Hz) as seen in Figure 32.

For comparison between guitars, a mean tone duration is obtained by averaging over all plugged tones where T15 is reliably calculable. Because of the increasing amplitude modulation at higher strings, only the four lower strings (E, a, d and g) are included in the average. The mean T15 for guitar Aa is calculated as 8.9 s. In comparison, guitar Cc has a mean T15 of 8.8 s. This nearly equal tone duration of both guitars suggests that the average decay cannot explain preference differences between guitar Aa and Cc in the listening test. However, the variation of the internal material damping, which was investigated in a separate study, might have an influence on the temporal behavior of a guitar, which could be described using the T15 calculation described above.

Another guitar quality attribute related to the decay could be the homogeneity of the tone duration or if single tone durations are below a certain T15 threshold. However, these attributes are probably difficult to hear with the strumming sequence used in the listening test. Therefore, they will not be further evaluated here.

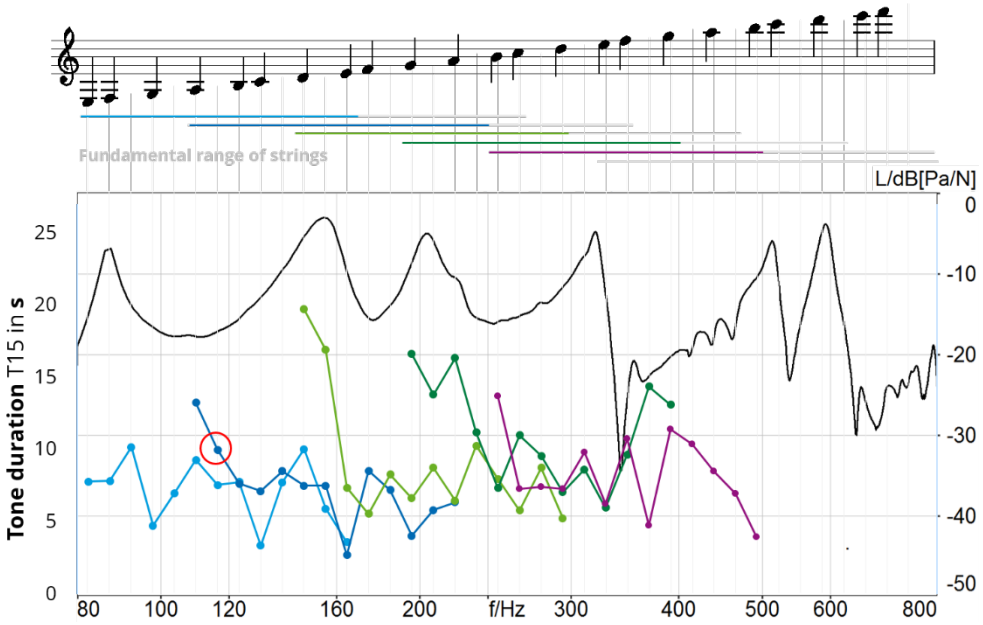

Figure 37 – Tone duration T15 calculated for 13 plugged tones of strings E (light blue) to b (purple). Marked with a red circle is T15 = 10 s for a# (a string) from the example above. For comparison, the measured transfer function is shown.

6 Summary

Acoustical properties of guitars with a fixed geometry but varying material parameters have been measured using different approaches. Reasons for the differences in guitar preference found in a listening test were analyzed by spectral analysis of recorded music sequences and the discussion of measured transfer functions. The most significant differences in the listening test could be linked to differences in the frequency response of the measured transfer functions. Specifically, the radiated energy in the bass range, and thus the overall tonal balance of the sound, appeared to have a strong effect. The amount of radiated energy seemed to depend mainly on the varying absolute frequencies of the strongly coupled resonances. These resonance frequency variations could be linked to varying material parameters of the wood. In addition to density and Young's moduli, the strong variation of shear modulus helped to explain the vibroacoustic behavior of the instruments. The findings underline the importance of wood selection based on material parameters if a fixed guitar design is given and a specific modal tuning is desired.

No influence of the density variation of the guitar tops on the overall level of the transfer functions and the resulting overall loudness/volume of a guitar was found.

A modal analysis revealed mode shapes of the soundboard linked to specific peaks in the transfer function. The strong influence of the frequency distance between these peaks and scale notes on the level and decay of tone partials was discussed. Then, a method to calculate a single value tone duration T15 was introduced, which will be used to analyze differences between guitars with varying internal material damping in part 4 of the report.

7 Appendix

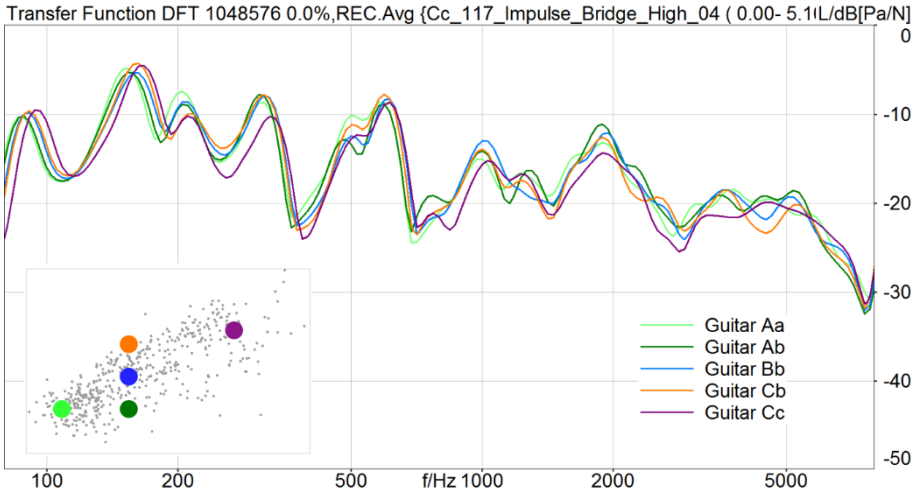

Figure 38 - Comparison all guitars in group 1 using the transfer function of the frontal microphone to the force input at the bridge.

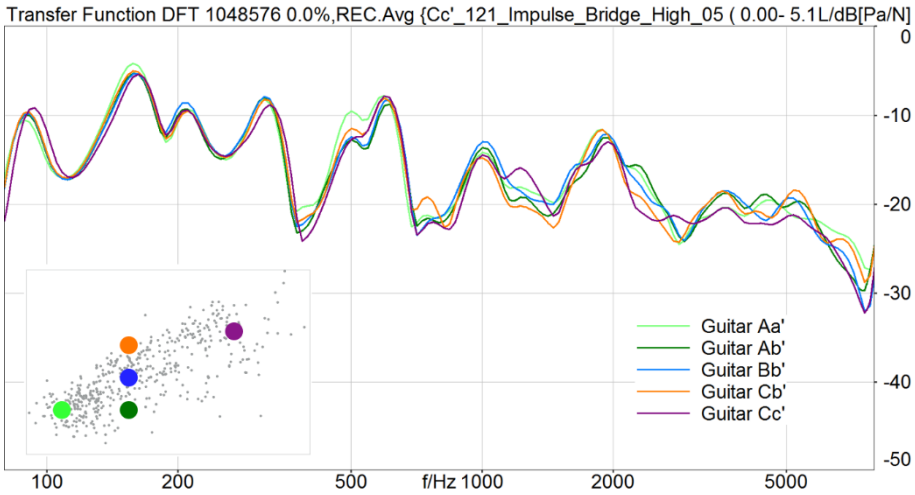

Figure 39 - Comparison all guitars in group 2 using the transfer function of the frontal microphone to the force input at the bridge.

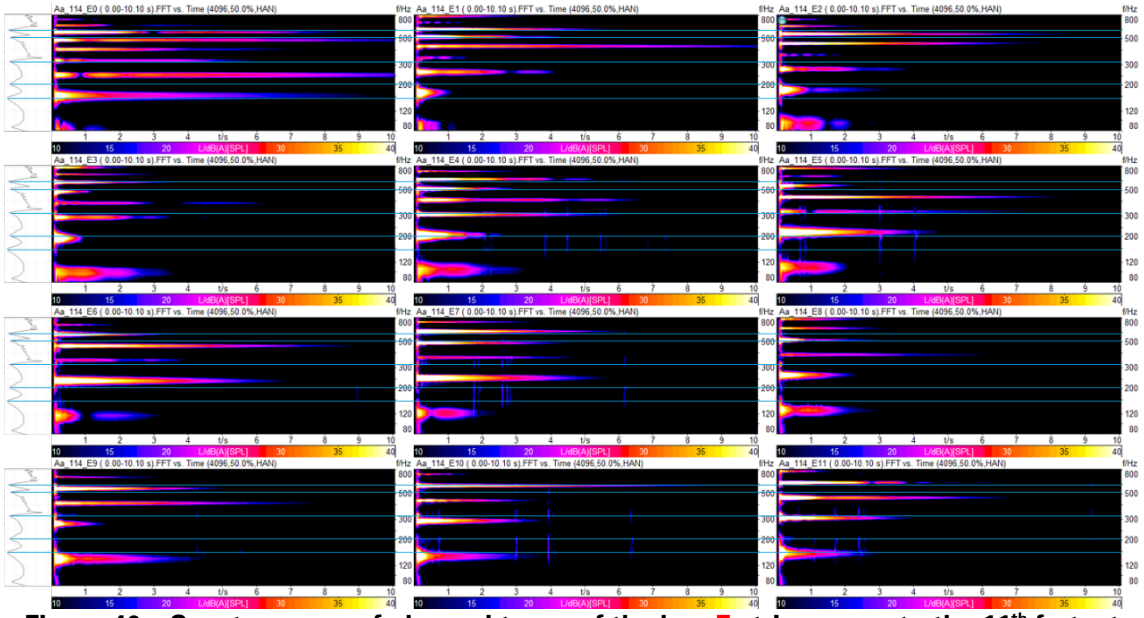

Figure 40 – Spectrograms of plugged tones of the low E string, open to the 11th fret, at the microphone positioned 2 m in front of the sound hole of guitar Aa. For comparison, the corresponding measured transfer functions are plotted on the left. Dominant resonance frequencies are marked with blue lines.

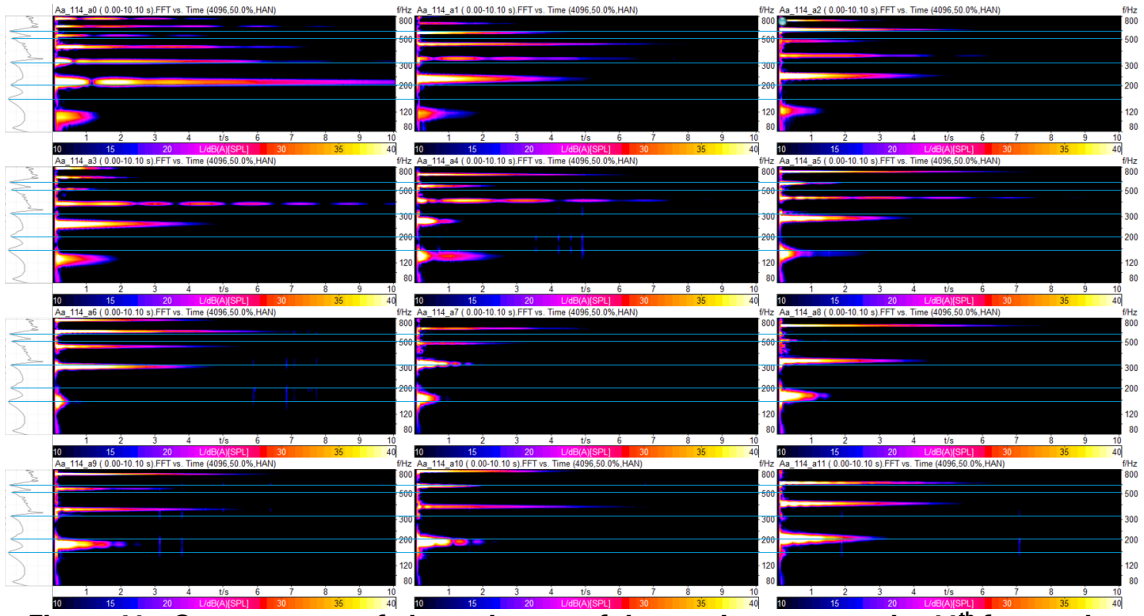

Figure 41 – Spectrograms of plugged tones of the a string, open to the 11th fret, at the microphone positioned 2 m in front of the sound hole of guitar Aa. For comparison, the corresponding measured transfer functions are plotted on the left. Dominant resonance frequencies are marked with blue lines.

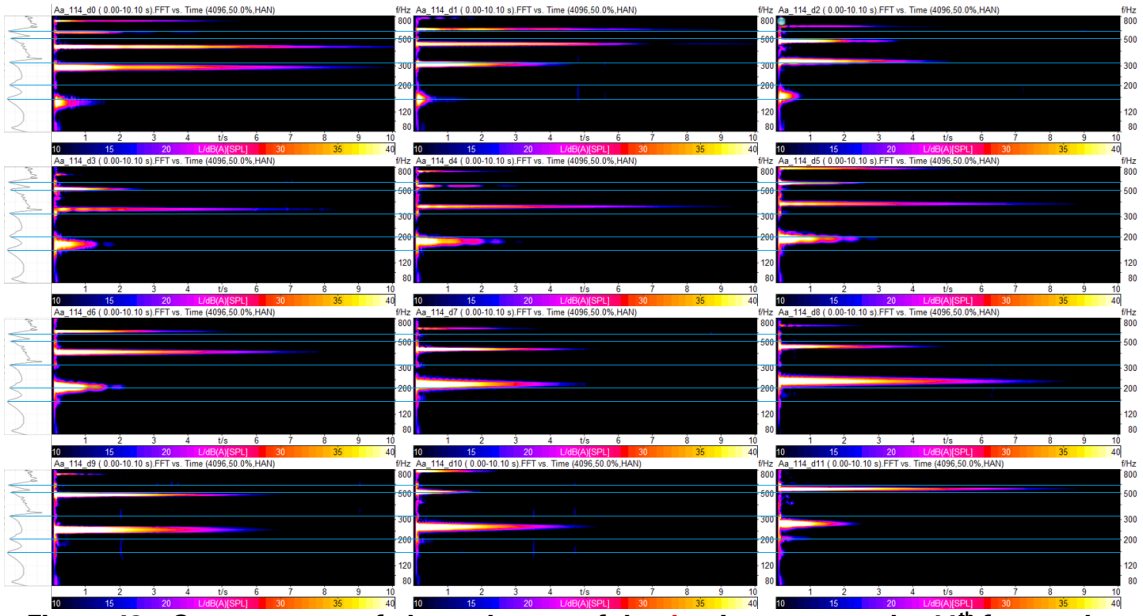

Figure 42 – Spectrograms of plugged tones of the d string, open to the 11th fret, at the microphone positioned 2 m in front of the sound hole of guitar Aa. For comparison, the corresponding measured transfer functions are plotted on the left. Dominant resonance frequencies are marked with blue lines.

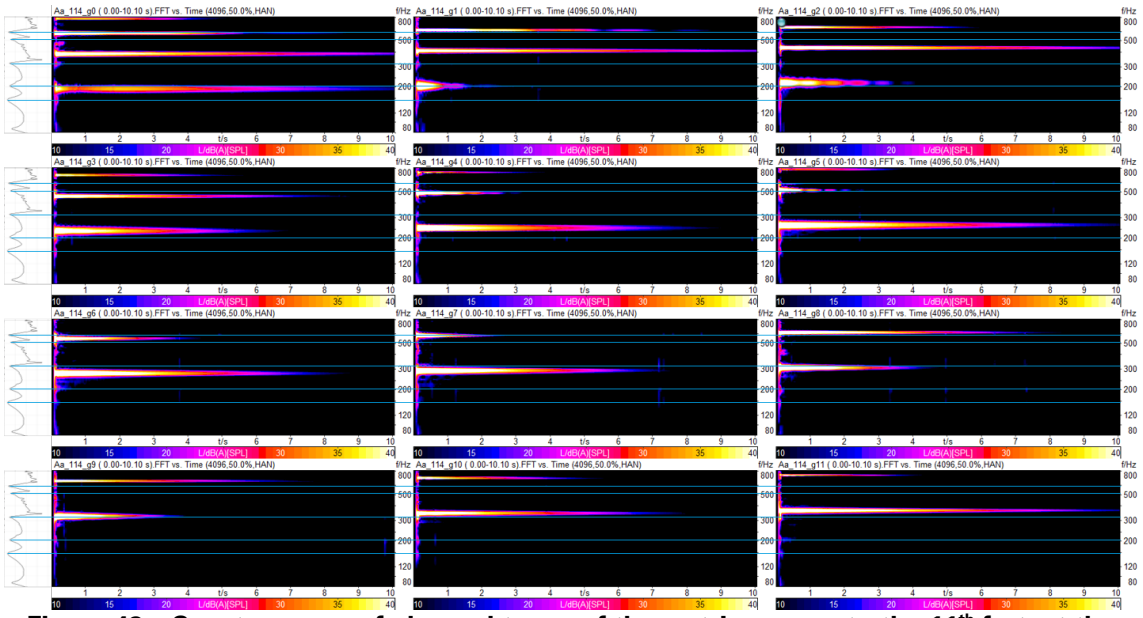

Figure 43 – Spectrograms of plugged tones of the g string, open to the 11th fret, at the microphone positioned 2 m in front of the sound hole of guitar Aa. For comparison, the corresponding measured transfer functions are plotted on the left. Dominant resonance frequencies are marked with blue lines.

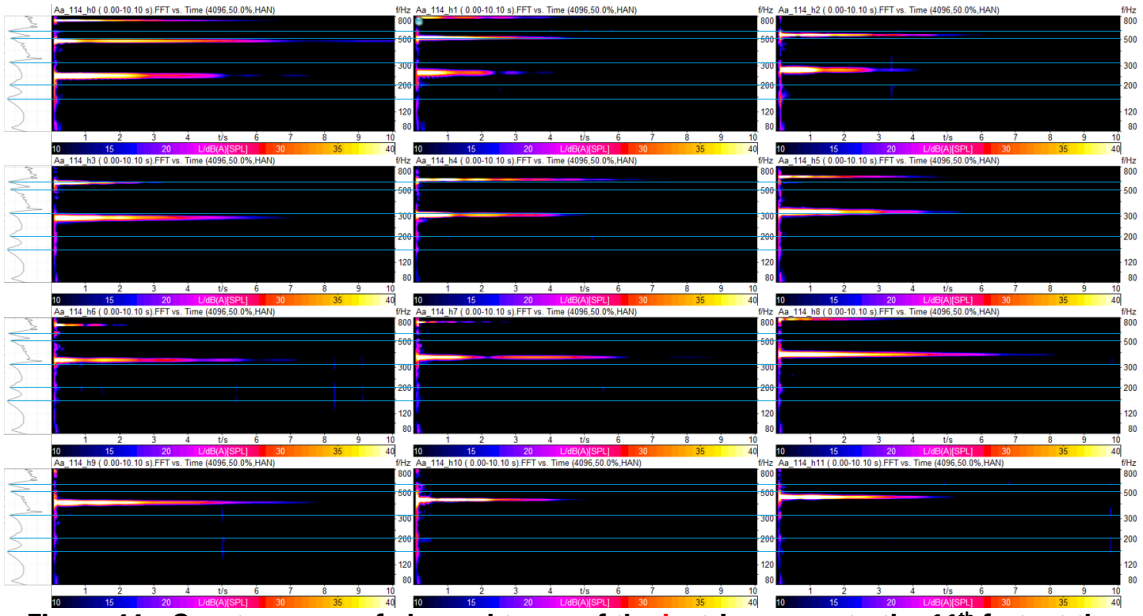

Figure 44 – Spectrograms of plugged tones of the b string, open to the 11th fret, at the microphone positioned 2 m in front of the sound hole of guitar Aa. For comparison, the corresponding measured transfer functions are plotted on the left. Dominant resonance frequencies are marked with blue lines.

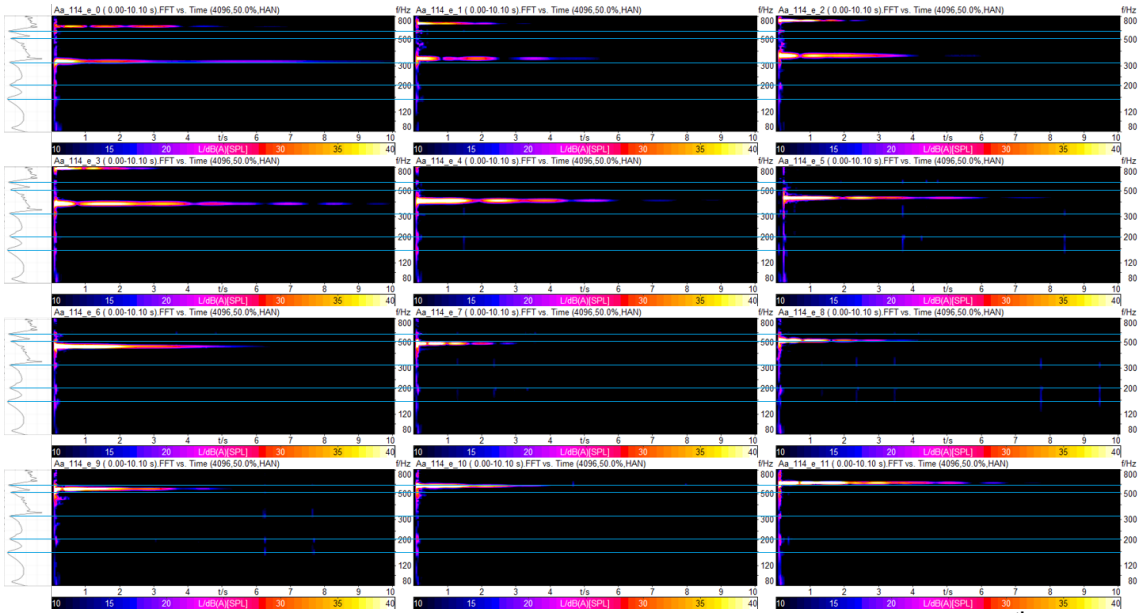

Figure 45 – Spectrograms of plugged tones of the high e string, open to the 11th fret, at the microphone positioned 2 m in front of the sound hole of guitar Aa. For comparison, the corresponding measured transfer functions are plotted on the left. Dominant resonance frequencies are marked with blue lines.

Literature

[1] Gore, Trevor, and Gerard Gilet. Contemporary Acoustic Guitar Design and Build: Volume 1; Design. Trevor Gore, 2016.